ELSEVIER

Journal of Power Sources 87 (2000) 212–217

JOURNAL OF POWER SOURCES

www.elsevier.com/locate/jpowsour

Charge–discharge characteristics of a solid-state Prussian blue secondary cell

M. Jayalakshmi, F. Scholz *

Institut für Chemie und Biochemie, Ernst-Moritz-Arndt-Universität Greifswald, Soldmannstraße 23, D-17489 Greifswald, Germany

Received 3 September 1999; received in revised form 19 November 1999; accepted 22 November 1999

Abstract

A solid-state secondary cell with Prussian blue, i.e., iron (III) hexacyanoferrate (II), as the active material of both the anode and cathode was constructed. The Prussian blue was mixed with graphite powder, potassium chloride and diluted hydrochloric acid to form a thick paste. A Nafion membrane was used as separator. The charge–discharge performance of the cell was studied in galvanostatic mode. For a stabilized cell, the cell voltage was invariably 1.0 V at half-discharge, whereas it varied from 2.0 to 1.0 V at half-charge depending on the charging rate. Double-step chronopotentiometric experiments were also carried out to understand the charge–discharge behaviour. The practical capacity was estimated to be 20 A h/kg from the maximum deliverable current on discharge. The cell was stable up to 60 cycles of charge–discharge and did not show any significant deterioration.

Keywords: Prussian blue; Solid-state secondary cell; Charge–discharge studies

1. Introduction

Prussian blue (PB), i.e., iron (III) hexacyanoferrate (II) is a well-known zeolitic compound, which has been investigated recently with regard to its applications to electrochromic displays [1–4], electrocatalysis [5–7] and ion-selective electrodes [8,9]. The high chemical reversibility of two distinct redox reactions of PB is its most important property. When electrochemically deposited on ITO electrodes, the PB film undergoes 10^5 cycles without deterioration [10]. Similarly, on a SnO_2 electrode, the PB film exhibits reversibility up to 10^7 cycles [11]. The chemical reversibility of the oxidation–reduction cycles is only associated with marginal changes of the crystal structure. It is also known to be highly stable in acidic solutions. Whereas alkali metal ions, preferably potassium, are easily sustaining the insertion electrochemistry, it has been shown [12] that protons can also be inserted and expelled upon reduction and oxidation of PB. However, in competition with potassium ions, this process is not favoured. These two characteristics of PB, i.e., reversibility and stability, make it attractive to study this material for battery applications. Few authors had attempted testing such application and the results of these studies are not conclusive because of the technical difficulties in handling the material.

A secondary cell with PB as both anode and cathode has been tried for the first time by Neff [13]. Taking into account, the reduction of high-spin iron (PB to Prussian white (PW) transition), which occurs at 0.195 V vs. SCE and the oxidation of low-spin iron (PB to Prussian yellow (PY) transition), which occurs at 0.87 V vs. SCE in 1 M K_2SO_4 solutions, he constituted a PB battery with PB as both anode and cathode. For a cell where half of the high-spin iron of the cathode is oxidized to $+3$ and half of the low-spin iron of the anode is reduced to $+2$, the theoretical cell voltage is 0.68 V. He deposited galvanostatically PB into porous graphite electrodes and used them as battery electrodes. The major problem encountered in this procedure was the lack of adherence of PB deposit on the carbon substrate. PB was lost as a finely dispersed sol from the electrodes after repetitive charging cycles, thus leading to the rapid loss of capacity per cycle. In another work [14], thin layers of hexacyanoferrates (*hcf*) of iron (Fe*hcf*, i.e., PB) and copper (Cu*hcf*) on platinum were used as anode and cathode materials in a secondary cell, taking aqueous potassium nitrate solution as electrolyte. At

* Corresponding author. Tel.: +49-3834-864450; fax: +49-3834-864451, +49-3834-864413.

E-mail address: fscholz@rz.uni-greifswald.de (F. Scholz).

0378-7753/00/$ - see front matter
PII: S0378-7753(99)00488-7

full charge, the maximum cell voltage obtained was 0.9 V and the films were stable up to 1000 cycles of charge–discharge without considerable drop in current efficiency but the coulombic capacity decreased to about 70% after 766 cycles. Interestingly, the duration of a charge–discharge cycle was within a time scale of 30 s. The failure of the cell after repetitive cycling was attributed to an overcharged Cu*hcf* layer and its degradation. In yet another approach [15], rechargeability of solid-state copper cells using PB and PY cathodes was studied. Cell voltage of Cu/PB cell was 0.58 V and that of the Cu/PY cell was 0.57 V and the maximum discharge capacities at 100 μA/cell were 1.35 and 1.98 mA h, respectively. The Cu/PY cell was reported to be relatively more stable over 700 cycles compared to that of Cu/PB cell.

In spite of the disadvantages exhibited by solid-state cells such as slow ionic or atomic diffusion and poor interfacial contact, they are inherently robust, spill-proof, and compact, and can be used over a wide temperature range. So various attempts were repeatedly made to improve the performance of solid-state cells by varying the electrode and electrolyte composition. It is essential that the electrode material should have an open pathway for the diffusing ions. This is the case for many compounds, e.g., Ag_xTiS_2 and TiS_2, which are successfully used as positives in secondary cells. Recently, some transition metal oxides of the type $LiNiO_2$, $LiCoO_2$, and $LiMn_2O_4$ are used as cathode materials for rocking chair batteries where carbon acts as anode. In all these cases, the reversibly intercalating cations between the anode and cathode are lithium ions and non-aqueous electrolytes are employed.

PB has an open structure for ion diffusion and it also has a sufficient electronic conductivity. In the present work, an attempt is made to use PB in a graphite-electrolyte paste as both anode and cathode material in a solid-state secondary cell and the charge–discharge characteristics are examined. Double-step chronopotentiometric experiments are also carried out to understand the charge–discharge behaviour. With PB being dispersed in a paste, it was supposed to overcome problems associated with the instability of PB films on solid electrodes.

2. Experimental

2.1. Materials

Commercial PB powder was used as obtained (HEYL chem.–pharm. Fabrik, Berlin, Germany). The powder X-ray diffraction pattern of the PB was that of insoluble form of PB, $Fe_4^{III}[Fe(CN)_6)_3]$ as reported, except for minor differences in the diffraction intensities. Graphite powder used as an auxiliary conductive agent was of analytical grade. Potassium chloride used along with PB and graphite powder was also of analytical grade and used as obtained. A Nafion membrane was used as separator.

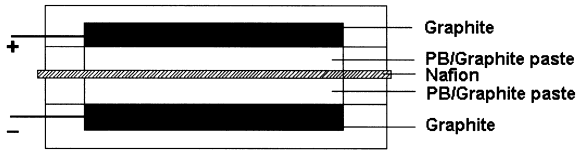

Fig. 1. Cross-sectional view of the PB/PB solid-state secondary cell.

2.2. Preparation of battery electrodes

In the PB/PB secondary cell as discussed earlier, both anode and cathode was made of a PB–graphite paste of the same composition. The electrodic mixture consisted of PB powder (0.5 g), graphite powder (1.7 g) and potassium chloride (0.5 g). This mixture was well ground in an agate mortar to form a paste with a few drops of dil. HCl (0.1 M). This particular composition was arrived at after trying various combinations of the ingredients and this ratio was found to be the most advantageous in the battery performance. The electrode mixture was then filled into a circular disc and the resultant electrode had a diameter of 14 mm and thickness of 4 mm for each compartment.

2.3. Cell design and configuration

The PB/PB cells had the configuration PB_m/Nafion/PB_m where PB_m denotes the mixture of PB, graphite, and KCl. Fig. 1 shows the cross-sectional view of the cell designed. Electrical contact is made from graphite (14-mm diameter, 4-mm thick) embedded into a polyacrylic block with dimensions of 24×24 mm^2 and 6 mm thickness. Nafion sandwiched between the two electrodes acted as a separator. Nafion also acted as an ion-exchange membrane, exchanging cations between the two electrodes, thus maintaining the charge balance and the insolubility of reduced and oxidised PB. The transferred ions were protons only.

2.4. Instrumentation

The cells were charged in the galvanostatic mode with an Autolab (ECO-Chemie, Utrecht, Netherlands). They were discharged by using a resistor, voltmeter, and multimeter by constant current discharge. The duration of each charge and discharge was 30 min and the cycling was performed without rest time. The change in cell voltage during charging and discharging was measured at intervals of 5 min.

3. Results and discussion

As assembled, the PB/PB cell showed prior to charging an open-circuit voltage (OCV) of 0.0 V. Throughout this study, the cell is charged and discharged in constant current mode. Frequently, secondary batteries are charged

at a rate C (Q_{the}/t) and discharged at lower rates, due to the incomplete conversion of the charging current into utilizable reaction products. In the present case, the rate C was calculated for the amount of PB taken to prepare the battery electrodes. In this calculation, the equivalent weight of the so-called soluble form of PB, $KFe_2(CN)_6$ was used (306.8 g/mol). This so-called soluble form of PB tends to form colloidal solution when the ionic strength is low, however, in the paste electrodes used in this study, no colloid formation has to be feared, as the electrolyte was saturated with KCl. As will be discussed below, the initial so-called insoluble PB, i.e., $Fe_4^{III}[Fe(CN)_6]_3$, is converted into the so-called soluble PB, i.e., $KFe^{III}[Fe^{II}(CN)_6]$, as a result of electrochemical cycling, because the iron (III) ions, which are initially present in the interstitials are replaced by potassium ions from the electrolyte. The theoretical coulombic capacity and energy density was calculated based on the equivalent weights of anode and cathode materials in the battery [16]. For a net weight of 0.5 g PB taken to construct both anode and cathode, the estimated charge is 157 A s and thus, the rate C for the PB/PB cell is calculated to be 0.087 A for the charging period of 30 min. It is necessary to understand the behaviour of PB electrodes under charging and discharging conditions in order to evaluate the performance of PB/PB cell. In the initial cycles, the cell was charged and discharged with lower rates to allow the system to stabilise. Rapid charging was reported [13] to lead to an initial ohmic resistance.

When the PB/PB secondary cell is charged, one of the PB electrodes undergoes oxidation-converting PB to PY, i.e., PY, which is accompanied by loss of potassium ions from PB. This electrode acts as the anode or negative electrode of the cell. The reaction is represented by the following equation:

$$\underset{\text{PB}}{\{KFe^{III}[Fe^{II}(CN)_6]\}} \rightarrow K^+ + e^- + \underset{\text{PY}}{\{Fe^{III}Fe^{III}(CN)_6\}}$$

(Braces denote solid phases.)

Simultaneously, in the other PB electrode, reduction of PB takes place, converting PB to PW. This is accompanied by insertion of potassium ions. This electrode acts as the cathode or positive electrode of the cell. The reaction is written as:

$$\underset{\text{PB}}{\{KFe^{III}[Fe^{II}(CN)_6]\}} + K^+ + e^- \rightarrow \underset{\text{PW}}{\{K_2Fe^{II}[Fe^{II}(CN)_6]\}}$$

The net cell reaction is:

$$2PB \rightarrow PW + PY$$

Upon discharge, polarity reversal takes place and the reactions proceed in the opposite direction. The formal potential of the couple PB ↔ PY is 1.17 V and that of PB ↔ PW is 0.02 V vs. SHE by considering the solid metal hexacyanoferrates [17]. The theoretical cell voltage for the half-charged state is 1.15 V. We have considered K^+ as the counter cation (in the above redox equations), which enter into, and exit from, the PB lattice to maintain charge neutrality. There is also the possibility that protons play the role of charge balancing cations. However, it is known that protons are only to a small extent involved when acidic potassium electrolytes are used [12]. In such case of mixed ion insertion, the formal potentials will slightly differ from the case of pure potassium insertion. The Nafion membrane can transport protons only, but the PB will accept mainly potassium ions. Since the Nafion membrane transfers protons only, the anode compartment will loose protons and the cathodic compartment will gain protons. To avoid any appreciable pH changes in both compartments, the KCl electrolyte was acidified with hydrochloric acid. This is important also because PB would dissolve when the electrolyte in the anodic compartment would become alkaline.

The expected changes in potential of the anode and cathode during charging and discharging are illustrated in Fig. 2A. As can be seen from this figure, the cell voltage is minimum at the initial stage of charging, then increases and changes only slightly around the half-charged state, and finally reaches a maximum value at the terminal end of charging. During discharging, this behaviour is reversed. At too high charging rates, the increase in cell voltage at the terminal end of charging may be associated

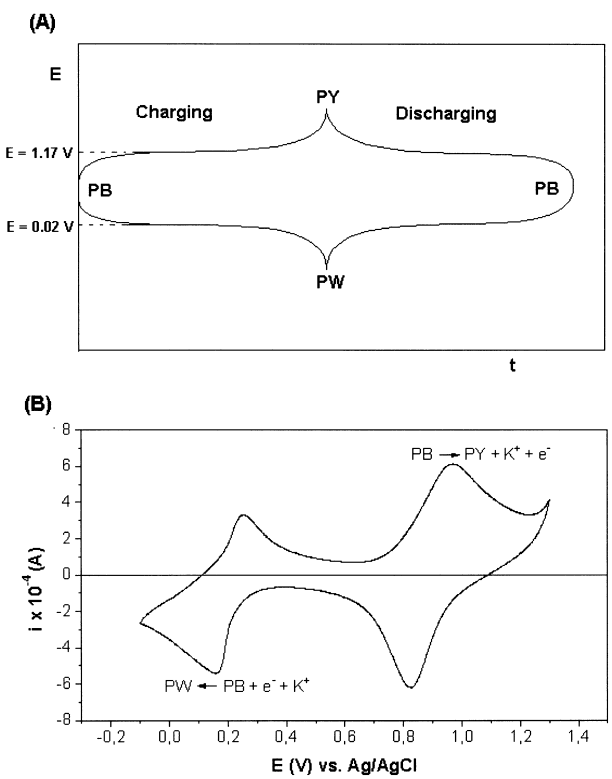

Fig. 2. (A) Theoretical curves illustrating the concurrent changes in potentials of the anode and cathode during (a) charging and (b) discharging of the PB/PB secondary cell. (B) Cyclic voltammogram of PB immobilised on a graphite electrode and using a KCl electrolyte.

with side reactions involving gas evolution. When a cell is overcharged, this undesirable situation may arise. Fig. 2B includes a cyclic voltammogram showing the two redox systems involved in the electrochemistry.

The first charge–discharge cycle of PB/PB cell is shown in Fig. 3, curves *a* and *a**. The cell is charged at *C*/17 rate and discharged at *C*/44 rate. As soon as charging is started, the cell picks up a voltage of 0.45 V and then gradually increases to reach a maximum of 1.18 V. During discharge, the cell voltage remains almost at a constant value of 0.56 V. The maximum available current for delivery on discharge, during this first cycle is very small. A h efficiency for rechargeable systems is defined as the ratio of discharge to charge capacities,

$$\text{A h efficiency} = \int i_{\text{dis.}}\,\mathrm{d}t / \int i_{\text{ch.}}\,\mathrm{d}t$$

The coulombic efficiency for this first cycle is only 40%. Though the cell reaches the value of theoretical cell voltage during charging, indicating that the conversion of PB to PW and PB to PY in both the electrodes takes place, the reverse is not found to be true as the cell voltage during discharge is only 0.5 V. This suggests that the cell is not yet stabilised.

The second charge–discharge cycle of PB/PB cell is shown in Fig. 3, curves *b* and *b**. The cell is charged at *C*/9 rate and discharged at *C*/17 rate. With increase in current values during charging, the cell voltage reached a maximum of 1.24 V. At this discharge rate, there is also an increase in cell voltage compared to that of the first cycle. However, a constant value of 0.84 V during discharge shows that the cell reactions are not equilibrated. The coulombic efficiency for this cycle is 50%.

The third charge–discharge cycle of PB/PB cell is shown in Fig. 3, curves *c* and *c**. Here, the cell is charged at *C*/6 rate and discharged at *C*/9 rate. Contrary to the initial two cycles, there is a dramatic increase in cell voltage during charging and the cell reaches a maximum voltage of 2.35 V. Without the benefit of three electrode cells, incorporating a suitable reference electrode, we are unable to determine, definitively with which electrode(s), this change is associated. Cell voltage at discharge, also improved as it varied from 1.08 to 0.94 V within the time scale of discharge. The coulombic efficiency of this cycle is 67%.

The fourth charge–discharge cycle of PB/PB cell is shown in Fig. 3, curves *d* and *d**. In this cycle, the cell is charged at *C*/4 rate and discharged at *C*/6 rate. The coulombic efficiency in this cycle is 75%. There are no appreciable changes in cell voltage during charging as well as in discharging. At full charge, the cell reached a maximum of 2.6 V. At discharge, the cell voltage varied from 1.08 to 0.94 as in the earlier cycle. This is almost a stabilised response of charge–discharge by PB/PB cell. The most probable reason for the increasing performance from cycle-to-cycle is the removal of oxygen from the electrode mixture by electrochemical reduction.

Fig. 4 shows the charge–discharge behaviour of the PB/PB cell in three different cycles of charge–discharge rates. The OCV of the cell prior to these experiments is noted to be 0.87 V. The cell is charged and discharged at *C*/7, *C*/11, and *C*/17 rates. The response of this stabilised cell is different from what we observed in the initial cycles. For example, the cell charged at *C*/17 rate reaches a maximum cell voltage of 1.47 V as against 1.17 V in the very first cycle (cf. Fig. 3, curve *a*). Similarly, for

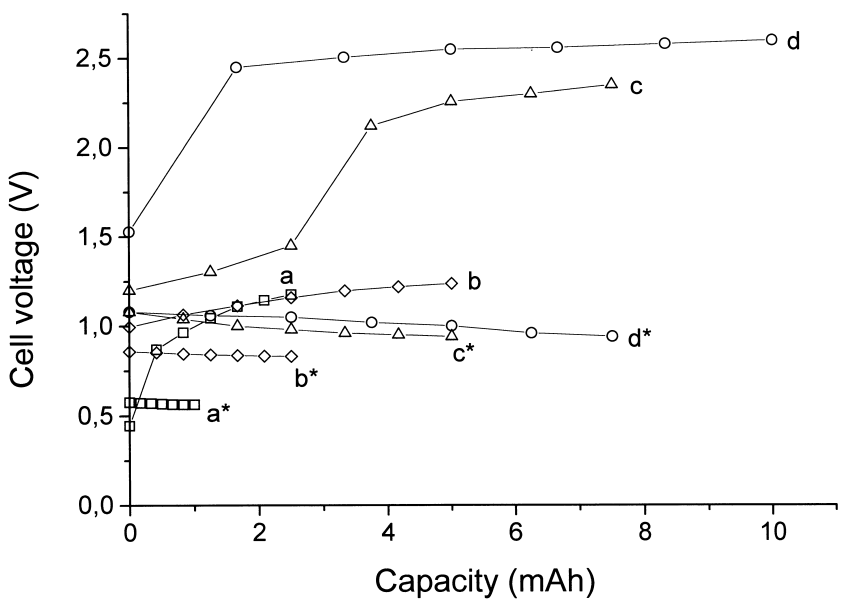

Fig. 3. Charge–discharge curves for the initial four cycles: (1) *a*, *a**; (2) *b*, *b**; (3) *c*, *c**; (4) *d*, *d** of the PB/PB solid-state secondary cell at different charge and discharge rates prior to stabilisation.

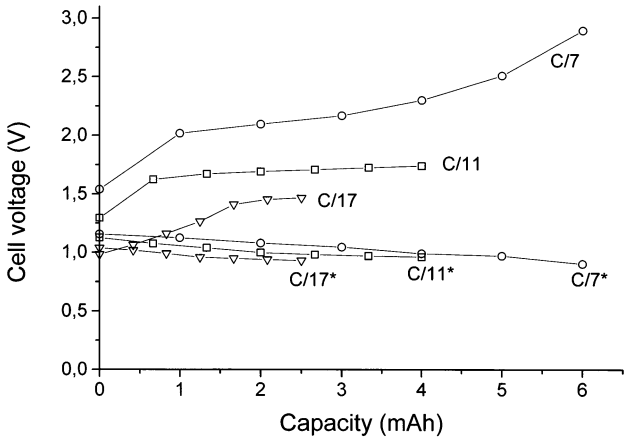

Fig. 4. Charge–discharge curves of the stabilised PB/PB cell at $C/17$, $C/11$, and $C/7$ charge and $C/17^*$, $C/11^*$, and $C/7^*$ discharge rates, respectively.

the same discharge rate, the cell maintained a constancy in cell voltage at 0.95 ± 0.05 V. Again, this result is different from the second cycle, where the cell voltage is only 0.84 V (cf. Fig. 3, curve b^*) for the same rate of discharge. For the charge–discharge cycle at $C/11$ rate, the cell voltage increased to 1.74 V but remained constant at 0.99 ± 0.05 V on discharge. With further increase in current on charging at $C/7$ rate, the cell reached a maximum of 2.89 V but on discharging at the same rate, the cell voltage varied significantly compared to the other two cycles. The variation is from 1.12 to 0.9 V, indicating that discharge at the same rate of charging especially at higher currents, shifts the cell voltage to lower values. Such subsequent deep discharge would require higher charging rate to bring back the cell to its initial capacity.

Fig. 5 shows the discharge curves of PB/PB cell at three different rates. After cycling the cell up to 60 cycles, the discharge behaviour of the cell at $C/9$, $C/7$, and $C/6$ rates are recorded. There is no noticeable difference in the lower discharge rate of $C/6$ where the terminal voltage is 0.98 V. But in the higher discharge rates, the cell voltage decreases to 0.87 and 0.8 V in the case of $C/9$ and $C/7$ rates, respectively. The fall in cell voltage on discharge seems to be more rapid than that of initial cycles of discharge.

In all these experiments, the cell voltage drops significantly from the end voltage of charging to the initial voltage of discharge. On changing the polarity of the electrodes for discharge, such drop in voltage is noticed invariably in all the cycles, irrespective of charge and discharge rates. For further understanding of such drop in cell voltage after charging, double-step chronopotentiometry of the PB/PB cell was carried out. Fig. 6 shows the results in curves *a* and *b*. Curve *a* is obtained by applying a positive current (5 mA) and curve *b* is obtained by applying a negative current (5 mA) to the cell. Curve *a* is the charging curve where the initial cell voltage starts at 0.94 V and increases to a terminal voltage of 1.97 V. The reverse curve *b* corresponding to the discharge curve starts at 1.68 V even if the experiment is continued without pause by the instrument. The cell voltage dropped by 0.29 V as the cell polarity is reversed. Theoretically, one should expect curve *a* to steeply ascend once the half-charged state is reached. The slowing down of the voltage increase above 1.5 V can only be understood to be due to a diffusion polarisation resulting from slow potassium ion diffusion in the PB. The fact that the electrode behaves very reversibly allows to exclude the presence of interfering redox processes, as these would be, most probably, very irreversible. Then, the sudden drop in voltage upon current reversal can be understood, as no diffusion polarization will occur at the beginning of discharging, since the most outer layer of the PY and PW particles will start to react.

The ability of the battery to retain charge without any self-discharge is very important for the long-term performance. This fact is reflected by the OCV of the cell, which corresponds to equilibrium values at designated states of discharge. In the PB/PB cell, the OCV, after a time

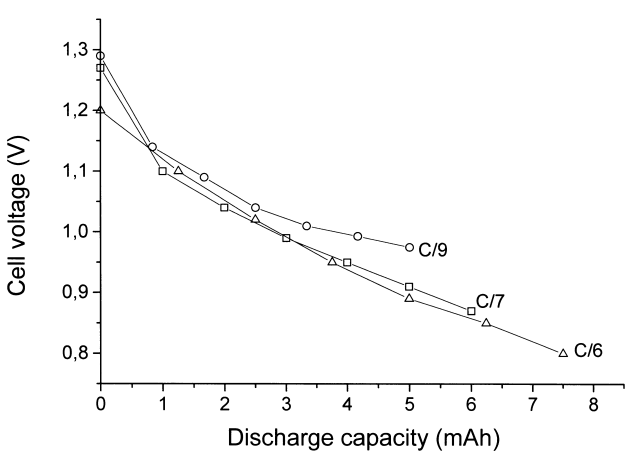

Fig. 5. Discharge curves of the cycled PB/PB cell at $C/9$, $C/7$, and $C/6$ rates, respectively.

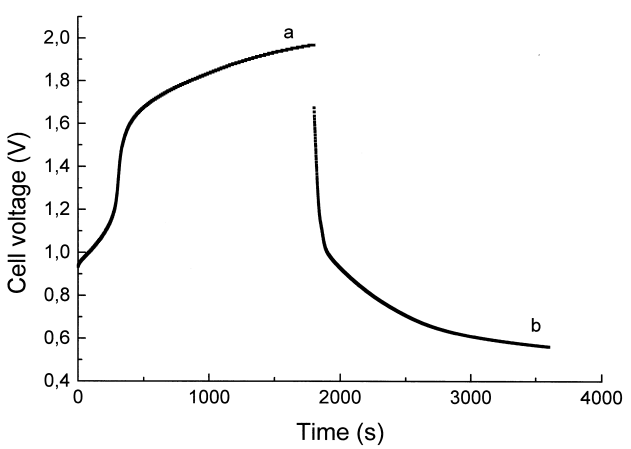

Fig. 6. Double-step chronopotentiometric curves obtained for the PB/PB cell (a) by applying 5 mA positive current (b) by applying 5 mA negative current in the time scale of 1800 s for each step.

interval of 5 to 10 min of discharge, is found to be around 0.9 V if there is continuous cycling of the cell. After 20 h in ideal state, the OCV of the cell drops to 0.76 V. Again, the cell is kept in ideal condition for 30 days and the OCV is checked. It is found to be 0.64 V. This kind of drop in voltage is reported to be due to self-discharge behaviour of the PB/PB cell, attributed to the presence or ingress of molecular oxygen, which reacts chemically with PW to form PB [18]. With a proper cell design, this deleterious effect can be avoided. Still, the cell is active to discharge on recharging as evident from Fig. 6, where the cut-off voltage is 0.56 V.

The theoretical capacity of the PB/PB cell is 87 A h/kg. With a thermodynamic cell voltage of 1.15 V, it gives a theoretical energy density of 100 W h/kg. The practical capacity of this cell is estimated to be 20 A h/kg by considering the maximum deliverable current on discharge. The energy density is 20 W h/kg and the cell voltage taken for this calculation is 1.0 V. From the ratio of practical to theoretical capacity, it is evident that only 1/4 of the PB taken is electrochemically active. The reason for this lack of electroactivity is not clear. Though the energy density is much smaller to the expected theoretical value, it is better than battery systems such as 1 M Fe–Cr or Ti^{3+}/Fe^{2+} redox couples in solutions, which are considered for off-peak power storage.

One significant drawback in this PB/PB cell was some electrolyte loss, which might be due to an insufficient cell construction. On continuous cycling, this led to a decrease in efficiency of the battery. After addition of few drops of water to the electrode, the cell regains its original capacity. This fact reveals that the ionic conductivity is the limiting factor in deciding the cell performance. The problem is rather technical than scientific. However, it cannot be excluded that some water loss is due to electrolysis, especially under high rate charging. Though the cell design has been meant to avoid the interference of molecular oxygen, it is found to be not completely immune to it. With a better cell design, these problems can be solved.

Acknowledgements

M.J. acknowledges provision of a fellowship from Alexander von Humboldt Foundation.

References

[1] H. Kellawi, D.R. Rosseinsky, J. Electroanal. Chem. 131 (1982) 373.
[2] K. Itaya, I. Uchida, S. Thoshima, R.M. De La Rue, J. Electrochem. Soc. 131 (1984) 2086.
[3] A. Viehbeck, D.W. Deberry, J. Electrochem. Soc. 132 (1985) 1369.
[4] K. Itaya, T. Ataka, S. Toshima, J. Am. Chem. Soc. 104 (1982) 3751.
[5] S. Sinha, B.D. Humphrey, A.B. Bocarsly, Inorg. Chem. 23 (1984) 203.
[6] K. Ogura, S. Yamasaki, J. Chem. Soc., Faraday Trans. 81 (1985) 267.
[7] F. Li, S. Dong, Electrochim. Acta 32 (1987) 1511.
[8] D. Engel, E.W. Grabner, Ber. Bunsen-Ges. Phys. Chem. 89 (1985) 9820.
[9] E.W. Grabner, D. Engel, Dachema Monogr. 102 (1986) 575.
[10] A. Roig, J. Navarro, J.J. Garcia, F. Vincente, J. Electroanal. Chem. 39 (1994) 437.
[11] K. Itaya, I. Uchida, Acc. Chem. Res. 19 (1986) 162, and references therein.
[12] N.F. Zakharchuk, B. Meyer, H. Hennig, F. Scholz, A. Jaworski, Z. Stojek, J. Electroanal. Chem. 398 (1995) 23.
[13] V.D. Neff, J. Electrochem. Soc. 132 (1985) 1382.
[14] E.W. Grabner, S. Kalwellis-Mohn, J. Appl. Electrochem. 17 (1987) 653.
[15] K. Kuwabara, J. Nunome, K. Sugiyama, Solid State Ionics 48 (1991) 303.
[16] E.J. Cairns, P. Shimotake, Science 164 (1969) 1347.
[17] F. Scholz, A. Dostal, Angew. Chem. 107 (1990) 2876.
[18] D. Ellis, M. Eckhoff, V.D. Neff, J. Phys. Chem. 85 (1981) 1225.